ELSEVIER

Desalination 129 (2000) 7–14

DESALINATION

www.elsevier.com/locate/desal

Characterization of fouling kinetics in ultrafiltration systems by resistances in series model

B. Tansel[a*], W.Y. Bao[b], I.N. Tansel[b]

[a]Department of Civil and Environmental Engineering and Drinking Water Research Center, [b]Department of Mechanical Engineering, Florida International University, University Park, Miami, FL 33199, USA
Tel. +1 (305) 348-2928; Fax +1 (305) 348-2802; email Tansel@eng.flu.edu

Received 6 October 1999; accepted 8 February 2000

Abstract

Membrane processes are gaining importance for water treatment applications as a result of the advances in membrane technology and increasing requirements on water quality. Membrane fouling, which results in loss of productivity, is one of the most important operational concerns of membrane processes. A number of theoretical models have been developed to explain membrane fouling mechanisms. These models use the system parameters (i.e., viscosity, pore size, membrane thickness, pressure) and unsteady-state material and flow balance equations with specific boundary conditions. As a result, they are of scientific interest and have limited use for practical applications. The purpose of the study was to develop a simple flux model to estimate the characteristic fouling times for ultrafiltration systems based on operational data. A simple first-order model was developed based on the resistances-in-series approach to correlate flux to a characteristic clean membrane parameter, system parameters. The model was used to estimate the characteristic fouling times of a laboratory ultrafiltration system.

Keywords: Membrane fouling; Flux; Water treatment; Ultrafiltration; Membrane processes; Resistances-in-series model; Membrane resistance

1. Introduction

Membrane processes have been used in water and industrial wastewater treatment applications for volume reduction of aqueous wastes, recovery of chemicals from liquid industrial wastes, desalination, drinking water purification [1–5] and removal of oil from oil–water emulsions [6,7]. Ultrafiltration (UF) and nanofiltration (NF) are pressure-driven treatment methods that separate contaminants based on size-exclusion. UF membranes typically have pore sizes in the

*Corresponding author.

0011-9164/00/$– See front matter
PII: S0011-9164(00)00046-1

range of 10 to 1000 Å. The pore sizes of the NF membranes are typically less than 1 nm (10Å). These processes differ from reverse osmosis (RO) and microfiltration (MF) based on the size range of the permeating species, mechanism of rejection, relative magnitudes of the permeate flux and the pressure differential across the membrane.

Membrane fouling, which results in loss of productivity, is one of the major operational concerns of membrane processes. The operational performances of the UF systems are often reported in terms of flux through the membrane. When a membrane is clean, the only resistance to flow is the membrane itself. However, as soon as the flow starts to permeate through the membrane, fouling begins and flux through the membrane gradually decreases as fouling progresses. A number of theoretical models have been developed to explain the fouling mechanisms of the membrane systems. Important models include resistances in series, gel-polarization, osmotic pressure, surface pore and hindered transport [5,8,9,10]. These models use the system parameters (i.e., viscosity, pore size, membrane thickness, pressure) and unsteady-state material and flow balance equations with specific boundary conditions. As a result, most often these models are of scientific interest with limited use for practical applications and interpretation of field data.

Objective of this research was to develop a simple model to characterize flux decline and to estimate the characteristic fouling times of membranes under specific operating conditions. A simple flux decline model was developed based on the resistances-in-series approach. The characteristic model parameters included a clean membrane resistance and a time-dependent resistance. The time dependent resistance was characterized by first-order kinetics. The model was tested using data from a laboratory scale UF system.

2. Model development

The fouling trends for UF membranes could be significantly different depending on the characteristics of the solution being filtered. For example, in drinking water treatment systems where the source water has relatively small concentration of contaminants, the flux decline follows a linear pattern. However, when the concentration of contaminants (or the compounds being separated) is high, the membrane flux shows an exponential decline. The flux decline can be attributed to concentration polarization, adsorption of contaminants within the membrane structure, pore blockage, and gel layer formation. Concentration polarization and gel layer formation take place primarily on the membrane surface where the pressurized source water is in contact with the membrane. Flux decline due to concentration polarization is reversible (i.e., can be removed by changing process parameters or by rinsing with water). However, flux decline due to gel layer formation is most often irreversible (i.e., requires chemical cleaning). Fouling caused by adsorption of contaminants and/or pore blockage within the membrane is most often irreversible, although fouling due to pore blockage could be partially reversible depending on the extent of blockage and blockage mechanisms between the contaminant and the pore openings of the membrane. Fig. 1 illustrates the different types of fouling mechanisms in relation to characteristics of the contaminants and the characteristics of the membrane.

Flux, which is defined as flow per unit area, is directly proportional to the driving force for flow and inversely proportional to the resistance to the flow. As a result, fouling of membranes by different fouling mechanisms could be represented as resistances-in-series through the membrane and above the membrane (i.e., cake layer), each resistance increasing with time resulting in a decline in the permeate flux [10]. The pressure-driven permeate flux through the

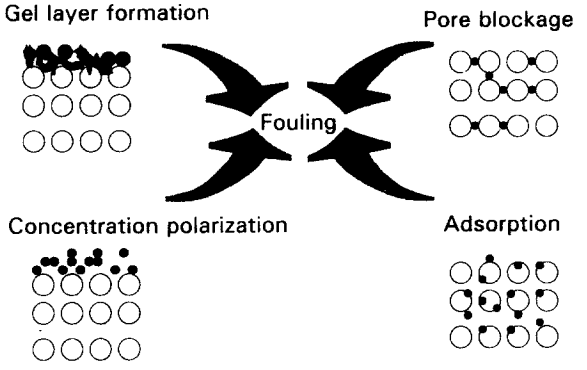

Fig. 1. Membrane fouling mechanisms.

cake layer and the membrane can be described by Darcy's law as follows:

$$J_v(t) = \frac{1}{A}\frac{dV}{dt} = \frac{\Delta p}{\eta_o (R_m + R_c)} \quad (1)$$

where J_v is the permeate flux (i.e., volumetric flux), V the total volume of permeate, A the membrane area, Δp the pressure drop imposed across the cake and membrane, η_o the viscosity of the suspending fluid, R_m the membrane resistance, and R_c is the cake resistance.

The osmotic pressure difference across the membrane can be significant as soon as the transport of solvent through the membrane begins. Then, the net pressure difference would be as follows:

$$\Delta P = \Delta p - \sigma \Delta \Pi \quad (2)$$

where ΔP is the net pressure difference across the membrane, σ the degree of permselectivity, and $\Delta\Pi$ is the osmotic pressure difference across the membrane.

Then, Eq. (1) can be written as

$$J_v(t) = \frac{\Delta p - \sigma \Delta \Pi}{\eta_o (R_m + R_c)} \quad (3)$$

As the flow goes through the membrane, fouling starts and R_c increases. During membrane filtration, it is very difficult to understand how the different fouling mechanisms work, and it is practically impossible to measure the extent of fouling caused by different fouling mechanisms. Since the flux from a membrane system for specific operating conditions (i.e., operating pressure) could be measured directly, a practical model can be developed based on the measurable variables of the system for specific operating conditions. Some parameters of the system that affect the flux are not time dependent (i.e., membrane type, and operating pressure). The change in flux can be correlated to the initial flux as follows:

$$\frac{J_v(t)}{J_{v0}} = \frac{(R_m + R_c)_{t=0}}{(R_m + R_c)_{t=t}} \quad (4)$$

or

$$J_v(t) = \frac{J_{v0}}{(R_m + R_c)_{t=t} / (R_m + R_c)_{t=0}} \quad (5)$$

A number of flux decline models have been developed based on assumptions for specific fouling mechanisms [11]. For example, a complete blocking model assumes that each particle arriving at the membrane participates in blocking the pores with no superposition of particles. This model is not a realistic representation of UF systems. The intermediate blocking model assumes each particle arriving at the membrane settles on another particle previously arrived and already attached on the membrane. According to the intermediate blocking model, time dependency of the system resistances can be represented as follows [11]:

$$(R_m + R_c)_{t=t} / (R_m + R_c)_{t=0} = (1 + At) \quad (6)$$

where $A = K_i J_{v0}$, and K_i is the blocked membrane area of flow per unit flow.

The standard blocking model assumes that the membrane consists of cylindrical pores of equal diameter and that each particle arriving at the membrane is deposited on the internal pore walls resulting in a decrease in flux. The standard blocking model can represent time dependency of the system resistances as follows [11]:

$$\left(R_m + R_c\right)_{t=t} / \left(R_m + R_c\right)_{t=0} = (1 + Bt)^2 \quad (7)$$

where $B = K_s J_{v0}$ and K_s is the decrease in the cross-sectional area of flow per unit flow.

The cake filtration model assumes that the particles arriving at the membrane attach on other particles already blocking the membrane and there is no room for directly obstructing some of the membrane area. By the cake filtration blocking model, time dependency of the system resistances can be represented as follows [11]:

$$\left(R_m + R_c\right)_{t=t} / \left(R_m + R_c\right)_{t=0} = (1 + Ct)^{1/2} \quad (8)$$

where $C = 2\ (R_c / R_0)\ K_c J_{v0}$, and R_c is the cake resistance, R_0 the clean membrane resistance and K_c the cake area per unit of total flow.

Depending of the characteristics of the membrane and the solution being filtered, these models represent the flow characteristics for a limited period of the operational cycle. Based on the flux curves developed from various industrial applications of UF systems and laboratory experiments, the overall trend of flux could range from a slow linear decline to a rapid exponential decline. When very dilute solutions are filtered, the pore blockage occurs very slowly. Since the contaminants do not block the pores uniformly, some pores may remain open for a long time. In field operations, the membranes are considered fouled when flux is reduced to 60% of the initial flux at which time the membranes are either cleaned or replaced. With the models presented above, it is difficult to predict the time when the membrane flux would decrease to 60% of the initial flux with reasonable accuracy.

During UF, the overall resistance to flow can be represented as a combination of two types of resistances: one time-dependent resistance which increases with time and another resistance which remains constant. The magnitudes of these resistances depend on the membrane characteristics and the characteristics of the solution being filtered. The increase in the magnitude of the time-dependent resistance can be represented by first-order kinetics. According to the first-order kinetic model, the fouling rate of membrane at any time is proportional to the extent of fouling already taken place. Then, the rate of fouling can be expressed as

$$\frac{d\alpha_t}{dt} = k\alpha_t \quad (9)$$

where k is the fouling rate and α_t the extent of fouling at time t.

Using the following boundary conditions: (1) at $t = 0$, $\alpha_t = \alpha$, (2) at $t = t$, $\alpha_t = \alpha_t$, then the magnitude of the time-dependent resistance can be expressed as

$$\alpha_t = \alpha e^{t/\tau} \quad (10)$$

Then the overall flux decline of a UF system can be represented in the following mathematical form:

$$\left(R_m + R_c\right)_{t=t} / \left(R_m + R_c\right)_{t=0} = (1 - \alpha) + \alpha e^{t/\tau} \quad (11)$$

where τ is the fouling time constant.

This general mathematical model for membrane fouling can be used to represent both the very slow fouling trends such as those

observed during drinking water treatment and the accelerated fouling trends observed during laboratory experiments.

By redefining the system parameters in Eq. (3):

$$a = \eta_o \alpha / (\Delta p - \sigma \Delta \Pi) \quad (12)$$

$$b = \eta_o \beta / (\Delta p - \sigma \Delta \Pi) \quad (13)$$

Eq. (3) can be written in a simplified form:

$$J_v(t) = \frac{1}{a + b e^{t/\tau}} \quad (14)$$

This model can easily be used to predict fouling time when the flux decreases to a specific percentage of the initial flux. For example, Eq. (11) can be rearranged to predict the time when the flux would decline to 60% of the initial flux as follows:

$$\left(R_m + R_c\right)_{t=t} / \left(R_m + R_c\right)_{t=0} = 0.60 = (1-\alpha) + \alpha e^{t/} \quad (15)$$

$$\alpha e^{t/\tau} = 0.60 - (1-\alpha) \quad (16)$$

$$e^{t/\tau} = [0.60 - (1-\alpha)] / \alpha \quad (17)$$

$$t/\tau \ln(e) = \ln[0.60 - (1-\alpha)] / \alpha \quad (18)$$

$$t = \frac{\tau \ln[0.60 - (1-\alpha)] / \alpha}{\ln(e)} \quad (19)$$

The general form of the Eq. (14) can also be used to interpret the normalized flux data. Flux data are normalized by dividing the instantaneous flux by the initial flux. For the normalized flux, the general flux equation would take the following form:

$$\text{Normalized flux} = \frac{J_i}{J_o} = \frac{a+b}{a+be^{t/\tau}} = \frac{1}{a_n + b_n e^{t/\tau}} \quad (20)$$

where $a_n = a/(a + b)$ and $b_n = b/(a + b)$. An important characteristic of this model is that the characteristics fouling time constant (t) would be the same for both the flux and the normalized flux curves.

3. Model verification

The simple flux model represented by Eq. (14) was verified with data collected from a series of test runs conducted using a laboratory scale UF system. The experiments were conducted using the same system and type of UF membrane but using contaminated water with significantly different fouling characteristics. To change the fouling mechanisms, the contaminant characteristics were altered by adding coagulants to feed water prior to UF. The addition of the coagulant destabilizes the colloidal particles and other organic contaminants (i.e., small oil droplets) in the mixture to form aggregates of a larger size. As a result, the particle size distribution in the source water changes. The experimental conditions and analytical methods used are described below.

3.1. Materials and methods

The UF experiments were conducted using a laboratory-scale continuous cross-flow membrane filtration unit manufactured by Desalination Systems, Inc. (DSI) (Escondido, California). The schematic of the experimental set-up is shown in Fig. 2. Test water in the feed tank could be first directed to a coarse filter primarily to remove large solids (if feed water contains floating or large solid particles) and to protect the pump. For the experiments the coarse filter was bypassed since the feed water did not

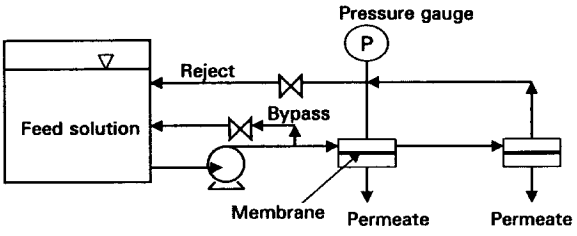

Fig. 2. Schematic of the ultrafiltration test set-up.

contain large solids. During the UF experiments, the feed water the water was recirculated back to the feed tank. The UF cell had a filtration area of 78.5 cm^2. The membranes used during the experiments were also manufactured by DSI and consisted of G-50 UF membranes with polyester backing and a permeate carrier layer. The molecular weight cut-off (MWCO) of the G-50 membranes was 10,000 Daltons. The general properties of G-50 membranes are provided in Table 1. Table 2 presents the characteristics of the laboratory-scale UF system used.

Contaminated pond water was used as the source water during the experiments. The pressure of the feed water was 100 psi. Table 3 presents the characteristics of the pond water before the addition of the contaminants. The pond water samples were contaminated with a mixture of regular unleaded gasoline, diesel fuel, and jet fuel in equal proportions by volume. The contaminated water samples were prepared at 3000 ppm concentration and distributed into 1-l Pyrex jars containing the pond water samples. The bottles were rotated for 24 h by a mechanical rotator to achieve equilibrium between oil and water phases prior to UF. The fuel oil mixture contained petroleum hydrocarbons ranging from C_7H_8 to $C_{21}H_{44}$. The UF experiments were conducted with and without the coagulants. To change the fouling characteristics of the contaminated water, two different coagulants were used. Based on the results of the coagulation experiments conducted using the jar test method, Cat floc T-2 and Cat floc K-10 were selected as the coagulants. Table 4 presents the physical and chemical properties of Cat floc T-2 and Cat floc K-10. Each membrane test was run for 8 h and 30 min. Initial feed water turbidity, pH and temperature readings were recorded.

Table 1
Characteristics of thin-film composite G-50 ultrafiltration membranes

Parameter	Value
Molecular weight cut-off, Daltons	15,000
Chlorine tolerance	High
Max. operating temp., °C	50
Applications	Oil–water separation Color removal from potable water, colloidal iron/silica removal RO pretreatment, industrial stream separations

Table 2
Characteristics of the laboratory-scale ultrafiltration system

Parameter	Value
Membrane diameter, cm	10
Membrane area, cm^2	78.5
Max. feed flow, l/min	4.6

Table 3
Characteristics of the pond water used for the test runs

Parameter	Quality
Turbidity, NTU	17 ± 2
Total solids, ppm	28 ± 6
pH	7.5 ± 0.1
Organics	ND

Table 4
Physical and chemical properties of Cat floc T-2 and Cat floc K-10

Parameter	Cat floc T-2	Cat floc K-10
Ingredients	Poly(dimethyldiallylammonium chloride)	Aluminum sulfate and poly-(dimethyldiallylammonium chloride)
Solubility in water	Complete	Complete
Specific gravity	1.072–1.112	1.19–1.25
pH, at 25°C	5.0–8.0	2.0–2.4
Percent volatility, w/w	~65	~77
Viscosity, cps at 25°C	74–275	20–75

4. Results

The coefficients of the model were determined using the experimental data. First, the model was calibrated using the data from the test runs with no coagulant use. Calibration involved primarily estimation of the coefficients a and b in Eq. (14). These two coefficients define the flux through a clean membrane. Coefficient a represents the resistance to the flow due to the presence of the membrane regardless of the extent of fouling. Coefficient b represents the component of the resistance, which increases as the membrane begins to foul. For a given membrane type and primary solvent (i.e., water), these coefficients would be the same. However, the rate of fouling would be different as the concentration or the characteristics of the contaminant in the solvent change. For the UF system used, the values of a and b were determined to be 0.085 and 0.624, respectively. For the UF test runs which were conducted using the coagulants Cat floc K-10 and Cat floc T-2, only the third coefficient (t) was estimated since the other two coefficients were determined by the model calibration. The filter model for the system used was found to be as follows:

$$J_v(t) = \frac{1}{0.082 + 0.625e^{t/\tau}} \qquad (21)$$

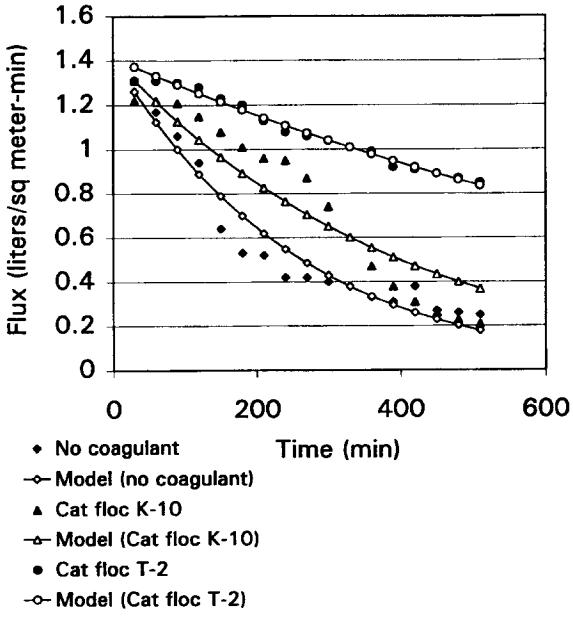

Fig. 3. Measured and estimated fluxes.

where t = 234 min when no coagulant is used, 335 min when Cat floc K-10 is used and 882 min when Cat floc T-2 is used.

The beginning resistance of the system was determined to be 0.707. The average errors in t were estimated as 6.5% for the test run with no coagulant, 11.6% for the test run using Cat floc K-10 and 1.7% for the test run using Cat floc T-2. Fig. 3 presents the data and estimated flux curves using the model provided by Eq. (21).

5. Conclusions

A simple model for flux decline in UF systems was developed based on the resistances-in-series model. A time-dependent resistance and a constant resistance were used to represent the resistances to the flow during filtration. The increase in the magnitude of the time-dependent resistance was represented by first-order kinetics. The model can easily be used to predict the critical fouling times when the flux decreases to a specified fraction of the initial flux. The model can also be used to interpret the normalized flux data. An important characteristic of the model is that the characteristics fouling time constant (t) would be the same for both the flux and the normalized flux curves. The model can be used to represent the flux trends for membrane systems with very slow linear decline as well as those with rapid exponential decline.

6. Symbols

A — Membrane area, m^2
J_v — Permeate flux (i.e., volumetric flux), m^3/m^2 s
k — Fouling rate, s^{-1}
K_c — Cake area per unit of total flow, m^2/m^3
K_i — Blocked membrane area of flow per unit flow, m^2/m^3
K_s — Decrease in the cross-sectional area of flow per unit flow, m^2/m^3
Δp — Pressure drop imposed across the cake and membrane, N/m^2
ΔP — net pressure difference across the membrane, N/m^2
R_m — Membrane resistance, m^{-1}
R_c — Cake resistance, m^{-1}
R_0 — Clean membrane resistance, m^{-1}
V — Total permeate volume, m^3

Greek

α_f — Extent of fouling, dimensionless
σ — Degree of permselectivity, dimensionless
$\Delta\Pi$ — Osmotic pressure difference across the membrane, N/m^2
η_o — Fluid viscosity, $N \times s/m^2$
τ — Fouling time constant, s

References

[1] J.C. MacNeil, CRC Crit. Rev Environmental Control, 18 (1988) 91.
[2] J.G. Jacangelo, J. Demarco, D.M. Owen and S.J. Randtke, J. Amer. Wat. Works Assoc., 87 (1995) 64.
[3] J.G. Jacangelo, J.-M. Laine, E.W. Cummings and S.S. Adham, J. Amer. Wat. Works Assoc., 87 (1995) 100.
[4] R. Rautenbach and R. Albrecht, Membrane Processes, Wiley, New York, 1989, pp. 272–332.
[5] A.S. Jonssön and G. Trägårdh, Desalination, 77 (1990) 135.
[6] J.C. Watters, D.G. Murrer, M. Fleischman and E. Klein, in: Liquid Membranes: Theory and Applications, ACS Symp. Ser. No. 347, R.D. Noble and J.D. Way, eds., American Chemical Society, Washington, DC, 1987, pp. 166–181.
[7] Y. Huang, B. Batchelor and S.S. Koseoglu, Hazardous Waste & Hazardous Materials, 11 (1994) 385.
[8] G.B. Van Den Berg and C.A. Smolders, J. Membr. Sci., 40 (1989) 149.
[9] W.S.W. Ho and K.K. Silkar, Membrane Handbook, Van Nostrand Reinhold, New York, 1992.
[10] S.S. Kulkarni, E.W. Funk and N.N. Li, in: Membrane Handbook, W.S.W. Ho and K.K. Silkar, eds., Van Nostrand Reinhold, New York, 1992.
[11] J. Jacob, P. Pradanos, J.I. Calvo, A. Hernandez and G. Jonsson, Physicochemical Engineering Aspects, 138 (1998) 173.